Photodisintegration of deuterium determined from the electrodisintegration process*

D. M. Skopik, Y. M. Shin, M. C. Phenneger, and J. J. Murphy, II
Saskatchewan Accelerator Laboratory, University of Saskatchewan, Saskatoon, Canada S7N OWO
(Received 17 April 1973)

The equivalent photon cross sections were extracted from deuteron electrodisintegration measurements over an energy range of 17 to 28 MeV. Proton angular distributions were measured at 12 photon energies and the total cross section determined with an experimental uncertainty of approximately $\lesssim$6%. The differential cross section at 90° c.m. was also measured. Satisfactory agreement is found between deuteron photodisintegration theory and our measurements. A comparison with other recent (γ, p) cross section measurements is made.

[NUCLEAR REACTIONS ^{2}H$(e,p)e'n$, measured $\sigma(E_p, \theta)$, extracted ^{2}H$(\gamma,p)n$.]

I. INTRODUCTION

The photodisintegration of the deuteron until recently was considered to be a reaction in which theory and experiment were in reasonable accord. For energies below 100 MeV, the comprehensive theory of Partovi[1] has superseded earlier calculations largely on the basis of including terms up to the dipole-octupole interference and the use of a realistic potential to describe the deuteron. Meson exchange and nuclear-structure effects which were neglected in the above calculations are not expected to be significant in the energy region considered ($E_\gamma < 30$ MeV) where $E1$ transitions dominate. Indeed, a recent calculation[2] considering admixtures of baryon resonances gave essentially the same total cross section predicted by Partovi.

The experimental total cross-section data prior to 1973[3] for $14 < E_\gamma \leq 35$ MeV are shown in Fig. 1. While the uncertainty (only statistical errors are shown) especially at lower photon energies is fairly large, with the exception of the results of Weissman and Schultz, the data are in fair agreement with the theory of Partovi which is given by the solid line. However, Tietze, Reich, and Trier,[4] who have measured the 90° differential cross section, and Baglin *et al.*,[5] in the most recent total-cross-section experiment, report measurements that are approximately 20% lower than theory near $E_\gamma = 20$ MeV.

In contrast the results of Skopik *et al.*,[6] in which the electrodisintegration cross sections were measured, are in good agreement with theory based on a simple model which reduces to the effective range theory. Although it was pointed out by Shin[7] that the theoretical cross section could be lowered by a slight readjustment in the P-wave phase shifts, it would nevertheless still be difficult to reconcile the discrepancy between the electrodisintegration and photodisintegration processes. Thus the disagreement between theory and experiment is not readily explainable and necessitates further investigation.

Moreover, from purely experimental viewpoints, the resolution of this discrepancy is of considerable importance since a large number of photodisintegration experiments have been normalized to Partovi's calculation.

In this paper measurements of the energy and angular dependence of protons resulting from the electrodisintegration of deuterium between 17 and 28 MeV are presented. Because of the experimental difficulties of using real photons, we have performed the experiment using electrons and have extracted the equivalent photon cross sections from the electrodisintegration data.

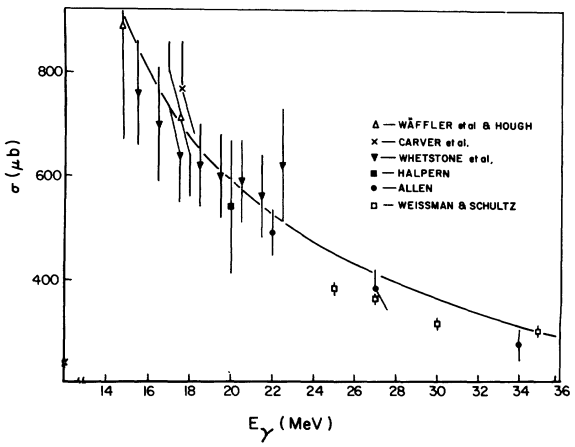

FIG. 1. Total-cross-section measurements of the ^{2}H$(\gamma,p)n$ reaction prior to 1973. The solid line is the calculation by Partovi.

II. EXPERIMENTAL ARRANGEMENT

The experimental apparatus consists of the University of Saskatchewan linear accelerator and spectrometer systems which have been described previously.[8,9] The spectrometer used in this experiment consists of five surface-barrier silicon detectors mounted in the focal plane of a 127° double-focusing magnet. The energy calibration for each detector was accomplished by varying the magnetic field and measuring the momentum distribution of α particles emitted from an ^{241}Am source located at the center of the scattering chamber. The midpoint of the momentum distribution determined the energy calibration. At higher energies the ^{1}H$(e,{}^1$H$')e'$ reaction in which the recoil protons were detected provided additional energy calibration points. The momentum calibration was found to be linear over the range of energies studied.

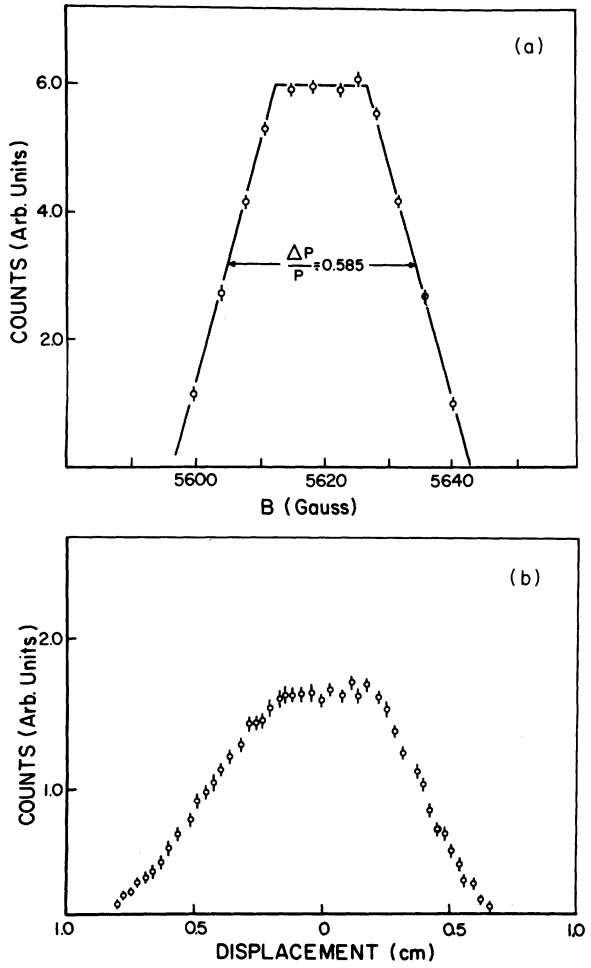

FIG. 2. α source measurements for detector 3: (a) momentum distribution of ^{241}Am α particles and (b) lateral efficiency measurement for $\theta_{spec} = 90°$ determined by moving the α source along the beam line.

To perform absolute experiments the product of spectrometer parameters which must be known is

$$\{\Delta\Omega_i \Delta E_i \eta_i\} n_t(\theta), \tag{1}$$

where $\Delta\Omega_i$, ΔE_i, and η_i are the effective solid angle, energy bite, and relative efficiency of the ith detector (note that η_i does not refer to the absolute counting efficiency which is 100%) and $n_t(\theta)$ is the effective target thickness in g/cm^2.

The term in braces was determined for the middle detector in the focal-plane array and the other detectors normalized to it. The energy bite $\Delta E_3 \sim 2\Delta P_3$ was found from the momentum distribution mentioned previously and is shown in Fig. 2(a). The solid angle was determined by the defining aperture of the magnet and thus could be ascertained purely by geometry for the middle detector since all other detectors were normalized to it. To verify this, the collimator size was varied and the count rate of ^{241}Am α particles was found to be proportional to collimator size over a range of sizes which included the collimator used in the experiment. The efficiencies η_i were found relative to η_3 by measuring at the same energy the protons from a BeO target. As a cross check the elastic recoil-proton spectrum for a fixed incident electron energy was measured with each detector and the resulting efficiencies were in agreement with those obtained from the BeO measurement.

In order to determine the effective target thickness seen by the spectrometer, the same α source was moved along the beam line with the magnetic field set at a constant value, corresponding to the calibration field of detector 3. The detected counts as a function of the position of the source was measured with the spectrometer at 90° with respect to the beam line. The resulting lateral efficiency of the spectrometer is shown in Fig. 2(b).

Because the target used in this experiment is an extended target, the effective target thickness is expected to vary with the spectrometer angle by

$$n_t(\theta) = \frac{n_t(90°)}{\sin\theta_{spec}} \tag{2}$$

TABLE I. Sources of error.

	Uncertainties (%)
Solid angle of the spectrometer	2.0
Incident electron flux	2.0
Momentum acceptance	2.0
Number of target nuclei	3.0
Real photon contamination	<0.5
Total	±4.6

since the effective path length of the spectrometer was appreciably smaller than the diameter of the gas cell.

In order to confirm the angular dependence of $n_t(\theta)$ and the accuracy of the product of parameters given by Eq. (1), recoil protons from the elastic scattering of hydrogen using an identical target cell were measured at three angles. The results were then compared with the proton elastic cross sections. To within the known uncertainties in the elastic proton data no deviations from Eq. (2) or in the absolute cross sections [which were found by using Eq. (1)] were observed.

The recoil protons were also used to obtain the multiple-scattering effects of protons from the disintegration of deuterons due to the gas and target wall. Although the multiple-scattering effects cannot be separated experimentally from the angular dependence of $n_t(\theta)$, it was found that measured elastic cross sections never exceeded the result of Drickey and Hand.[10] Hence the upper limit of the determination of the effective target thickness and multiple-scattering effects is that of the known elastic cross section.

In Table I we give the results and associated errors of the various measurements on the spectrometer.

The signals from the silicon detectors were amplified and fed into five analog-to-digital converters (ADC) associated with an XDS 920 computer. The ADC's were gated on for 4 μsec by the master accelerator trigger pulse corresponding to the arrival of each beam burst. A typical pulse-height spectrum is shown in Fig. 3.

A deuterium gas was contained in a right circular cylinder of 2.54-cm radius and 3.5-cm height. The walls were 0.000 64-cm Havar[11] foil. Since the vertical beam size was typically 1 mm, the vertical height of the gas cell imposed no background problems. The target cell was designed to be filled to a pressure of 2.0 atm and permanently sealed during the course of the experiment. A check for target leakage was periodically performed by measuring the recoil deuterons from elastic scattering. No leakage was discernible. Measurement of the elastic electron spectrum from the gas cell used in the experiment revealed target impurities of less than 0.2%.

The spectrometer entrance was masked so that the spectrometer would not accept protons produced in the target wall. The absence of tritons, deuterons, and α particles from the pulse-height spectra, even at extreme spectrometer angles, is evidence that all the proton yields are indeed free of wall contamination. Furthermore, when an evacuated target was placed in the beam, no protons could be detected at the extreme angles.

As a check for photon contamination in the electron beam a stacked-foil experiment was performed. No discernible photon contamination was observed in the primary electron beam. The estimate of photon contamination in Table I was made considering the target wall and gas as the source for real photons.

The beam current was monitored by a nonintercepting SLAC-type ferrite monitor.[12] The response of this monitor was checked periodically with a Faraday cup and was found to be reproducible and linear throughout the experiment.

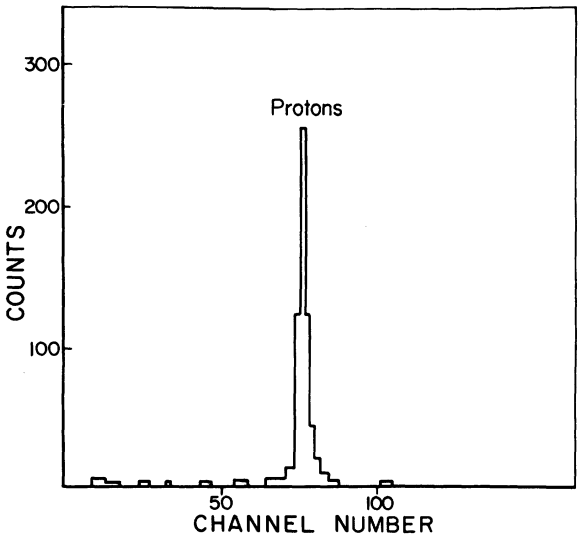

FIG. 3. A typical proton spectrum.

III. DATA ANALYSIS AND RESULTS

For a given spectrometer angle and proton energy the measured cross section is given by

$$\frac{d^2\sigma}{d\Omega_p dE_p} = \frac{C_p(\theta, E_p)}{\Delta E_p \Delta\Omega_p n_t(\theta)}, \tag{3}$$

where $C_p(\theta, E_p)$ is the number of protons per inci-

TABLE II. Angular-distribution coefficients (μb/sr) of the form $d\sigma/d\Omega = A_\gamma + B_\gamma \sin^2\theta + C_\gamma \sin^2\theta \cos\theta + D_\gamma \sin^2\theta \cos^2\theta$ at $E_\gamma = 20.0 \pm 0.25$ MeV.

	A_γ	B_γ	C_γ	D_γ	σ_{tot} (μb)
Partovi	5.4	61.3	18	4.2	588
Solution of Eqs. (7)	4.8 ± 2.1	63 ± 2	26 ± 1	7.8 ± 1.2	604
Using Eqs. (8) for the virtual photon spectrum	4.0 ± 2.2	64 ± 2	30 ± 1	10 ± 2	605
Baglin *et al.* [a]	2.8 ± 0.9	55 ± 2	20 ± 4	(4.2) [b]	502

[a] Reference 5.
[b] Assumed Partovi's value.

dent electron and ΔE_p and $\Delta\Omega_p$ are the energy acceptance and solid angle of the spectrometer, and $n_t(\theta)$ is the number of target nuclei per cm^2 as defined previously.

The energy transfer was computed under the assumption that the final electron scattered at zero degrees. At low incident electron energies this is a reasonable approximation since the cross section, because it is predominantly transverse, is weighted by $1/q_\mu^4$ where q_μ is the four-momentum transferred. This $1/q_\mu^4$ dependence favors forward scattering of the electrons. One identifies the energy transfer as the equivalent photon energy and writes the photon cross section as

$$\frac{d\sigma}{d\Omega}=\frac{C_p(\theta,E_p)}{\Delta\Omega n_t(\theta)N(E_0,E_\gamma)dE_\gamma/E_\gamma}, \tag{4}$$

where E_γ is the equivalent photon energy and $N(E_0,E_\gamma)dE_\gamma/E_\gamma$ is the virtual photon spectrum associated with ΔE_γ. $N(E_0,E_\gamma)$ depends on the multipolarity of the transition involved, but the usual procedure in extracting photodisintegration cross sections from electrodisintegration experiments is to consider only the dominant multipole. For the deuteron the error introduced by using only the $E1$ virtual photon spectrum is expected to be quite small since the reaction is predominantly $E1$. However, rather than neglect the dependence of the photon spectrum upon the multipolarity involved, we have considered in the data analysis all multipoles up to and including $E2$ and $M1$. For S-state nuclei one finds[13] that if the photon cross section is written as

$$\left.\frac{d\sigma}{d\Omega}\right|_\gamma = A_\gamma + B_\gamma\sin^2\theta + C_\gamma\sin^2\theta\cos\theta + D_\gamma\sin^2\theta\cos^2\theta \tag{5}$$

then,

$$\left.\frac{d\sigma}{d\Omega}\right|_e = A_e + B_e\sin^2\theta + C_e\sin^2\theta\cos\theta + D_e\sin^2\theta\cos^2\theta, \tag{6}$$

where

$$\left.\frac{d\sigma}{d\Omega}\right|_e = \frac{C_p(\theta,E_p)}{\Delta\Omega n_t(\theta)dE_\gamma/E_\gamma}$$

and

$$\begin{aligned}
A_e &= \frac{\alpha}{\pi}\{A_\gamma[(1+R_E^2)\lambda - 2R_E] + B_\gamma R_E^2 \\
&\quad + D_\gamma R_k^2(\tfrac{1}{3} - \tfrac{2}{3}R_E + \tfrac{1}{3}R_E^2)\}, \\
B_e &= \frac{\alpha}{\pi}\{B_\gamma[(1+R_E^2)\lambda - 2R_E - \tfrac{3}{2}R_E^2] \\
&\quad + D_\gamma R_k^2(\tfrac{1}{6}R_E - \tfrac{1}{12}R_E^2)\}, \\
C_e &= \frac{\alpha}{\pi}\{C_\gamma[(1+R_E^2)\lambda + R_k(-1 + \tfrac{1}{2}R_E + \tfrac{11}{6}R_E^2)]\}, \\
D_e &= \frac{\alpha}{\pi}\{D_\gamma[(1+R_E^2)\lambda + R_k^2(1 + \tfrac{5}{3}R_E - \tfrac{25}{12}R_E^2)]\},
\end{aligned} \tag{7}$$

with

$$\lambda = \ln\frac{2E_0(E_0-E_\gamma)}{m_e E_\gamma},$$

$$R_E = \frac{E_0-E_\gamma}{E_0},$$

$$R_k = \frac{E_0-E_\gamma}{E_\gamma}.$$

Thus by fitting the electrodisintegration cross section to the form given by Eq. (6), the corresponding photon coefficients can be obtained by solving the set of Eqs. (7).

As pointed out by Gibson and Williams[14] and Kundu, Shin, and Wait[15] the presence of the $E0$ multipole in electrodisintegration which is absent when real photons are used, can introduce some model dependence in the extraction of the equivalent photon cross sections. Since the ratio of the $E1/E0$ virtual photon spectra varies approximately

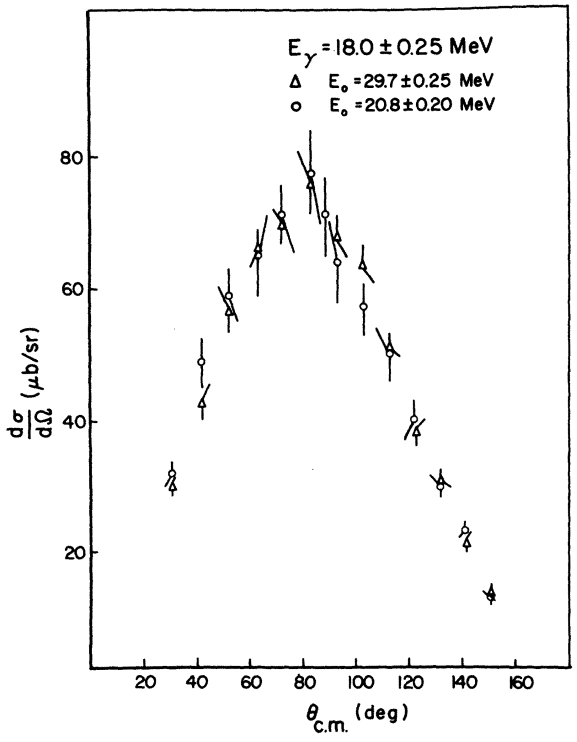

FIG. 4. Angular distribution of protons at E_γ = 18.0 ± 0.25 MeV for two incident electron energies.

as

$$\ln\left[\frac{2E_0(E_0-E_\gamma)}{m_e E_\gamma}\right] \Big/ \left[4\,(E_0-E_\gamma)^2/E_\gamma^2\right],$$

a test of possible model dependence in the extraction of an equivalent photon cross section was performed by measuring an angular distribution at $E_0 = 20.8$ MeV and comparing to the angular distribution measured at 29.7 MeV, which was the incident energy employed during the experiment. This kinematically reduces the $E0$ photon spectrum by 90%. The result of the measurement shown in Fig. 4 yielded a ratio

$$\frac{\sigma_{\rm tot}(E_0 = 29.7\ {\rm MeV})}{\sigma_{\rm tot}(E_0 = 20.8\ {\rm MeV})} = 1.00 \pm 0.09$$

indicating a lack of model dependence in the extraction of the equivalent photon cross section. Since the $E0$-$E1$ interference results in a $\cos\theta$ dependence in the angular distribution, the data were also fitted to the form given by Eq. (6) including a $\cos\theta$ term. The value of this coefficient was found to be consistent with zero over the entire energy range. However, since the $\cos\theta$ term can arise from Coulomb effects, it was not considered to be significant in the photon angular-distribution coefficients. Also, since the virtual photon spectrum used is only valid for the long-wave approximation, we have estimated using a simple model for the $E1$ nuclear matrix element, that the maximum error in using the long-wave approximation is less than 2%. This error was not used in computing the total error given in Table I.

Angular-distribution data were taken at 12 photon energies. In addition since Partovi tabulates the angular-distribution coefficients at 20.0 MeV, an angular distribution covering 19 angles was measured for $E_\gamma = 20.0 \pm 0.25$ MeV with particular emphasis on the extreme angles. The angular distribution at 20.0 MeV is shown in Fig. 5. Partovi's calculation in approximation I is given by the solid curve, which agrees quite well with this experiment. Table II gives the coefficients of the angular distribution at 20 MeV as determined from this experiment, Partovi's coefficients, and those measured by Baglin. Also given are the coefficients obtained when the virtual photon spectrum in Eq. (4) is taken as

$$N(E_0, E_\gamma) = \frac{\alpha}{\pi}\,\frac{\{R_E^{\,2} + [(1+R_E^{\,2})\lambda - 2R_E - \frac{3}{2}R_E^{\,2}]\sin^2\theta\}}{\sin^2\theta}. \tag{8}$$

Since the cross section is predominantly $E1$, the use of the $E1$ virtual photon spectrum is a reasonable approximation and yields essentially the same coefficients as obtained by solving the set of Eqs. (7). The experimental results are in good agreement with Partovi.

Figure 6 gives the total-cross-section results determined from least-squares fits to each of the

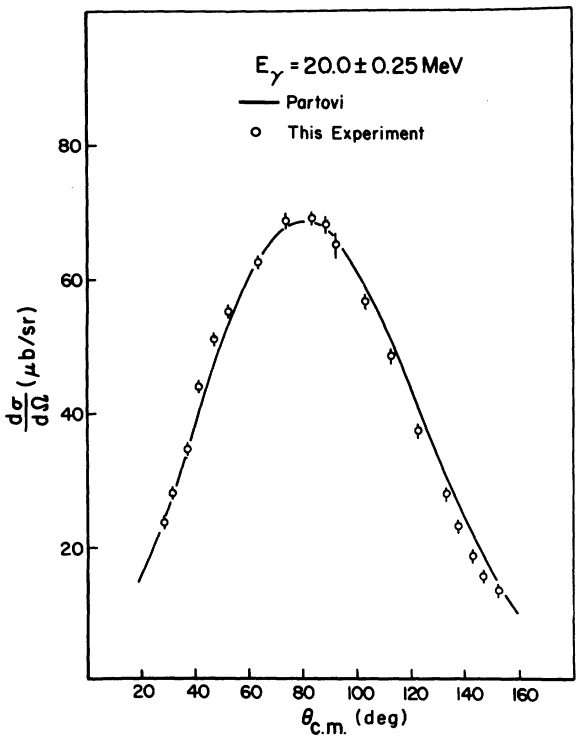

FIG. 5. Angular distribution of protons at $E_\gamma = 20.0 \pm 0.25$ MeV. The solid line is the prediction of Partovi.

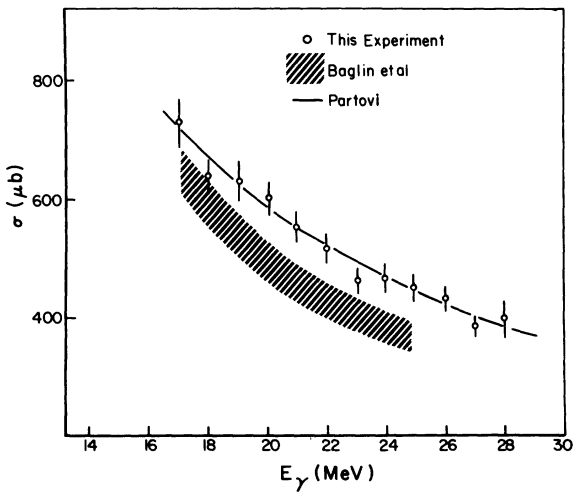

FIG. 6. Total cross section for the $^2{\rm H}(\gamma,p)n$ reaction showing our results, those of Baglin *et al.* (Ref. 5), and Partovi's calculation. The total error is shown for both experiments.

TABLE III. Total-cross-section results determined from the angular-distribution data combined in 1.0-MeV intervals. Error assigned to each point is the total error determined by adding the percentage statistical and systematic errors in quadrature.

E_γ (MeV)	$\sigma \pm \Delta\sigma$ (μb)
17.0	730 ± 42
18.0	640 ± 31
19.0	637 ± 31
20.0	604 ± 29
21.0	554 ± 26
22.0	496 ± 24
23.0	460 ± 23
24.0	465 ± 23
25.0	445 ± 22
26.0	430 ± 21
27.0	377 ± 20
28.0	400 ± 29

angular-distribution data combined in 1.0-MeV intervals. The results of Baglin *et al.* are also presented. The errors shown are the total errors for both sets of data. Our results are also tabulated in Table III.

As a further comparison a 90° differential cross section was obtained from Partovi's results by fitting the tabulated coefficients to a power series of the form $1/x^t$. The cross section is given by the solid line in Fig. 7 with our measured value of the differential cross section. The experimental results are in good agreement with Partovi.

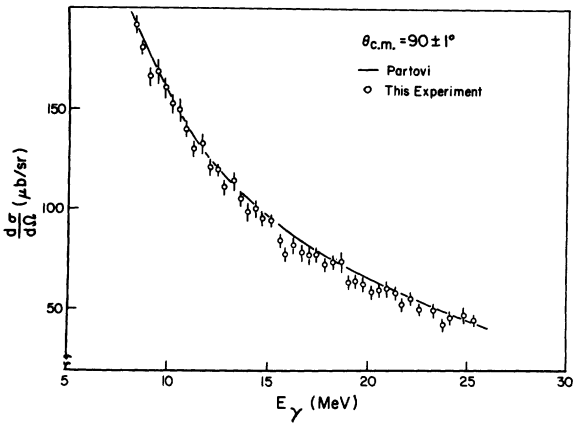

FIG. 7. Differential cross section at a c.m. angle of 90 ± 1°. The errors shown are statistical only.

IV. CONCLUSION

Over the energy range covered, reasonable agreement exists between this experiment and the total-cross-section calculation of Partovi. In particular, the experimental determination of the $E1$ coefficient (which is the main source of disagreement with the experiment of Baglin *et al.*) is in accord with that predicted by Partovi.

ACKNOWLEDGMENTS

We wish to thank Dr. L. Katz for his interest in this work, and R. Ehman for assisting with the data analysis.

*Work supported by the Atomic Energy Control Board of Canada.

[1]F. Partovi, Ann. Phys. 27, 79 (1964).
[2]H. G. Miller and H. Arenhovel, Phys. Rev. C 7, 1003 (1973).
[3]B. Weissman and H. L. Schultz, Nucl. Phys. A174, 129 (1971); H. Wäffler and S. Younis, Helv. Phys. Acta 24, 483 (1951); P. V. C. Hough, Phys. Rev. 80, 1069 (1950); J. H. Carver and D. H. Wilkinson, Nature 167, 154 (1951); C. A. Barnes, J. H. Carver, G. H. Strafford, and D. H. Wilkinson, Phys. Rev. 86, 359 (1952); A. Whetstone and J. Halpern, *ibid.* 109, 2072 (1958); L. Allen, Jr., *ibid.* 98, 705 (1955).
[4]K. Tietze, H. Reich, and J. O. Trier, Z. Phys. 242, 328 (1971).
[5]J. E. Baglin, R. W. Carr, E. J. Bentz, Jr., and C. P. Wu, Nucl. Phys. A201, 593 (1973).
[6]D. M. Skopik, Y. M. Shin, K. F. Chong, M. C. Phenneger, and E. L. Tomusiak, Phys. Lett. 43B, 481 (1973); K. F. Chong, M. C. Phenneger, Y. M. Shin, D. M. Skopik, and E. L. Tomusiak, Nucl. Phys. (to be published).
[7]Y. M. Shin, in International Conference on Photonuclear Reactions and Applications, Asilomar, California, 1973, edited by B. L. Berman (Ernest O. Lawrence Livermore Laboratory, University of California, Livermore, California, 1973), p. 345.
[8]L. Katz, G. A. Beer, D. E. McArthur, and H. S. Caplan, Can. J. Phys. 45, 3721 (1967).
[9]Y. M. Shin, D. M. Skopik, and G. D. Wait, Nucl. Instrum. Methods 94, 381 (1971).
[10]D. J. Drickey and L. N. Hand, Phys. Rev. Lett. 9, 521 (1962).
[11]Trademark, Precision Metals Division, Hamilton Watch Company, Lancaster, Pennsylvania.
[12]D. Olsen, Stanford Linear Accelerator Center, Technical Note No. SLAC-TN-65-66, 1965 (unpublished).
[13]J. J. Murphy, II, Ph.D. thesis, University of Illinois at Urbana-Champaign, 1971 (unpublished).
[14]B. F. Gibson and T. W. Williams, Nucl. Phys. A163, 193 (1971).
[15]S. K. Kundu, Y. M. Shin, and G. D. Wait, Nucl. Phys. A171, 384 (1971).